



DAMAGE VARIATION IN TYPICAL BRIDGE PIERS WITH DIFFERENT DAMAGE CONDITION AND WITH STEEL JACKETS

M. Consolación Gómez-Soberón

Professor, Materials Department, Universidad Autónoma Metropolitana, México DF, México
cgomez@correo.azc.uam.mx

Cesar Cruz-Martínez

Graduate student, Structures Master, Universidad Autónoma Metropolitana, México DF, México
cesar_cruz_mtx@hotmail.com

Edgar Tapia-Hernández

Professor, Materials Department, Universidad Autónoma Metropolitana, México DF, México
etapiah@correo.azc.uam.mx

David De León-Escobedo

Professor, Universidad Autónoma del Estado de México, Toluca, México
daviddleonescobedo@yahoo.com.mx

ABSTRACT: Some authors consider that the adequate rehabilitation technique for bridge piers is related to the current damage condition of these elements. In this paper, the analysis of the probabilistic damage variation that can be developed in bridge piers when they are under seismic load and show different damage levels is presented. To do that, for an existing bridge, a nonlinear model was constructed and calibrated with experimental data. For this model, the uncertainty on the mechanical properties of materials and earthquake loading was considered, based on accelerograms registered close to the bridge location. For the selected bridge, fragility curves were evaluated by Monte Carlo simulation and the most vulnerable elements were characterized. Based on the original model, damaged models were elaborated by considering some damage states for the most vulnerable pier. Light, moderate and severe damage levels were simulated by reducing the area of the concrete transversal section and rebar steel elements, according to information from experimental data. Finally, fragility curves were defined for bridge piers when the damaged element is rehabilitated with steel jackets, considering that the fragility curve of the element was close to the original curve, when the element was not damaged. Fragility curves are compared for all conditions.

1. Introduction

Fragility curves are decision tools that are used to define maintenance and rehabilitation programs. For the former, more vulnerable element or system are characterized to define the optimal rehabilitation procedure of the damaged structure. Fragility curves are obtained for various procedures; ones of the most used in recent years are the probabilistic analytical methods. The stochastic methods with Monte Carlo simulation and artificial records are used to define fragility functions, as by Nasseradiet *al.*, (2009). Fragility curves were defined by Liao y Loh (2004) for bridges in Taiwan, by analyzing reported damages. Karim and Yamazaki (2000) define fragility curves for typical bridges in Japan through a damage indices formulation. Nielson and DesRoches (2007) used limited functions, like the lognormal distribution, to characterize demand and capacity of bridge elements and, then, to obtain fragility curves for bridges in the United States. Zhang *et al.*, (2008) define fragility curves for several bridge configurations, including girder-to-pier connection, abutment type or the existence or not of isolation elements, by using stochastic evaluations. In addition, Mackie and Nielson (2009) evaluated the influence

of different uncertainties in the fragility curves evaluation by applying probabilistic tools. Padgett and DesRochehes (2008) obtained fragility curves for reinforced bridges, by considering these curves as tools to find out the best rehabilitation technique. Olmos *et al.*, (2014) analysed the seismic response of bridges with substructure rehabilitated with steel jackets, considering probabilistic estimations. Other papers indicated that fragility curves were used as useful decision tools for maintenance and rehabilitation programs. However, in Mexico only recent work has been dedicated to evaluate fragility curves for typical highway bridges, to formalize a reliable database.

In other aspects, designers do not have complete information to decide what is the best rehabilitation technique for bridge piers, since some authors think that the best rehabilitation technique depend on the element damage state. Then, in this paper, fragility curves of elements and systems of a common bridge configuration in Mexico were evaluated. Starting from these curves, some damage levels were assumed in the most vulnerable element and fragility curves were defined again. Finally, for every damaged bridge, steel jackets were used to rehabilitate bridge piers and fragility curves were evaluated. The comparison of all fragility curves were used to reach some recommendations.

2. Fragility curves of the original structure

2.1. Selected bridge

An existing structure was selected to define the damage variation of bridge piers, considering a typical Mexican highway typology. The chosen bridge, named Motín de Oro, is a continuous concrete structure with four spans of 25.15 m, 29.65 m, 29.90 m and 25.15 m, with a total length of 109.85 m. The bridge has three-single RC bent piers of 4.11 m, 4.26 m and 4.46 m, with a wall-box transversal section, as can be observed in Figure 1. The superstructure is a unicellular prestressed box girder of 10 m by 1.8 m of transversal and vertical dimensions, based on elastomeric bearings. Motín de Oro bridge was repaired in 1994 by using external and longitudinal cables, as shown in Figure 1; however, fragility curves were evaluated for the original condition. An experimental campaign was carried out to define the main dynamic characteristics of the structure. The two first periods of this structure are of 0.342 s and 0.276 s in longitudinal and transversal directions, respectively.

Motín de Oro bridge was modeled in SAP 2000 code (2000) because this software offers more tools to model bridge structures, like the ones to define bearings elements. The SAP model was calibrated with experimental data. In addition, the structure was modeled for the Ruaumoko-3D program (Car, 2004), to perform the nonlinear analysis and define the damage of piers. SAP and Ruaumoko models of the Motín de Oro bridge can be observed in Figure 2. The nonlinear analysis required interaction and moment-curvature diagrams for piers, which are the only elements with a nonlinear behaviour (superstructure was assumed elastic). These curves were defined by assuming uncertainty on the mechanical properties of the materials, as will be commented later. Additionally, Takeda model was applied to define constitutive laws of elements, and columns ductility was defined by using the Priestsley and Park (1989) expression

$$\mu = \left[\frac{3\phi_{\max}}{\phi_y - 1} \right] \left[\frac{L_p}{L} \right] \left[\frac{1 - 0.5L_p}{L} \right] \quad (1)$$

where L_p is the plastic hinge length, L is the distance between the column base and the center of mass of the superstructure, ϕ_y and ϕ_{\max} are, respectively, the yield and maximum curvature at the column base. Equation 1 assumed that the horizontal earthquake load acts in the system center of mass.

2.2. Uncertainty on mechanical properties and earthquake loading

Various accelerograms were selected to simulate artificial records, by considering seismic stations close to the bridge location (close to the Pacific Coast, one of the regions with the highest seismic hazard in Mexico). Of these stations, four seismic scenarios were defined as a function of PGA, magnitude and duration values. Selected accelerograms were: 1) January 11th, 1997, with PGA=396 cm/s²; 2) October 12th, 1995, with a PGA=227 cm/s²; 3) April 30th, 1986, with PGA=69.2 cm/s²; and 4) September 19th, 1985, with PGA=140 cm/s², the record with larger duration of the intense phase. Accelerograms and elastic spectra of the four records, for a 5% of critical damping, for the horizontal direction with greater values, are shown in Figure 3. As it is observed, the fundamental periods of the accelerograms are less than 0.5 s. Therefore, the two fundamental periods of the bridge are in the zone of larger amplitude of the

spectrum. Based on the signals of Figure 3, artificial records were generated by seeking similar velocity spectrums and keeping in mind that the accelerogram is formed by the sum of an infinite number of sine functions, with random phase angle between 0 and 2π . In addition, Table 1 shows the considered random mechanical variables with their assumed probabilistic distribution functions and the associated parameters, both taken from the available literature.

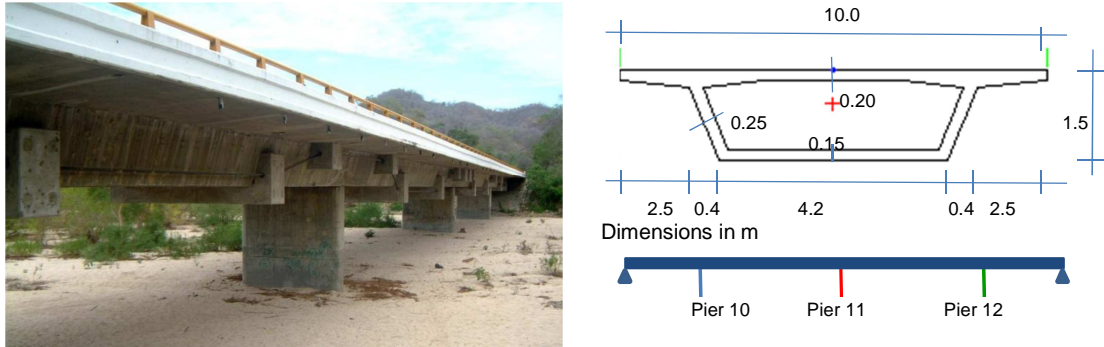


Figure1– Motín de Oro bridge and girder section

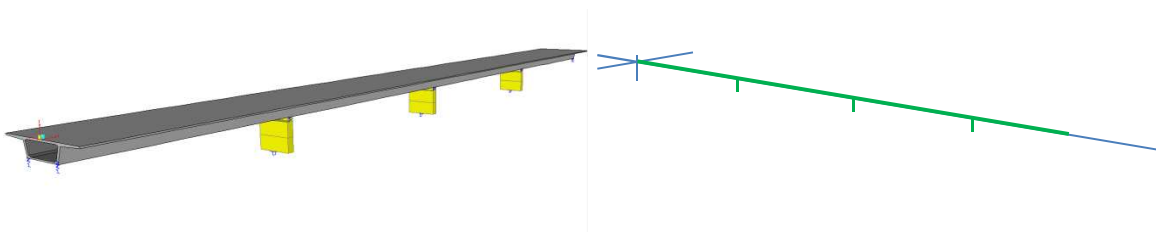


Figure 2– Motín de Oro SAP (left) and Ruaumoko (right) models

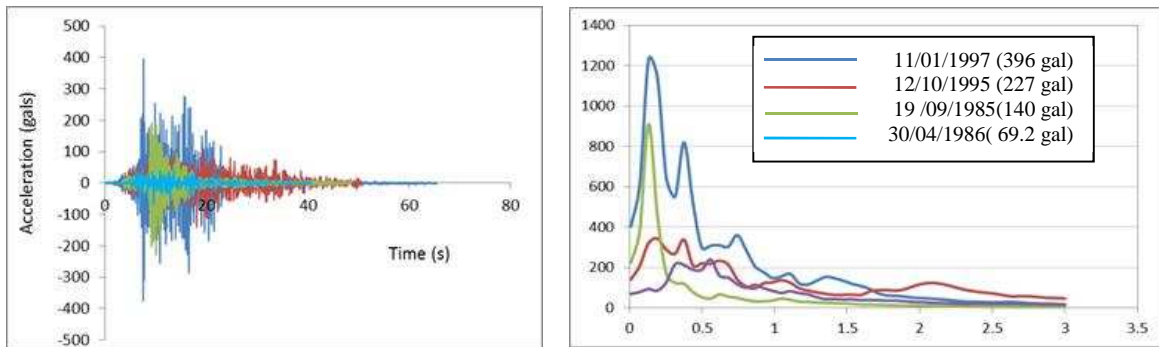


Figure 3– Accelerograms (left) and elastic spectrums (right) for the largest horizontal component of the four seismic scenarios

Table 1 – Probabilistic models of the mechanical properties

Variable	Description	Mean	CV	Distribution
f'_c (KPa)	Concrete compressive strength	28890	0.064	Normal
E_c (KPa)	Concrete elastic modulus	22000000	0.077	Lognormal
w_c (KN/m ³)	Concrete specific weight	24	0.040	Normal
f_y (KPa)	Steel yield stress	412020	0.064	Normal
f_u (KPa)	Steel ultimate stress	618030	0.064	Normal
E_s (KPa)	Steel elastic module	210000000	0.080	Lognormal
w_s (KN/m ³)	Steel specific weight	77	0.010	Normal

2.3. Fragility curves

The uncertainty of external load was included with artificial accelerograms, for the described seismic scenarios and for the mechanical properties with the distribution functions shown in Table 1. Monte Carlo simulation technique was employed to define fragility curves of Motín de Oro bridge. In this process, 300 variations of the nonlinear analyses by each seismic scenario were used to define local and global damage indices. The number of variations analyses was defined by considering that the mean value of the results is nearly constant when it is close to 300. The damage indices formulation used in this work was the one proposed by Park *et al.* (1985), because it is simple and it has an exhaustive calibration with experimental test. Local (for elements) and global (for a system) damage indices proposed by Park *et al.* are expressed as

$$ID = \frac{\delta_m}{\delta_u} + \frac{\beta}{F_y \delta_u} \int dE \quad (2)$$

$$ID_G = \frac{\sum_i ID_i^2}{\sum_i ID_i} \quad (3)$$

where δ_m and δ_u are, respectively, the maximum and ultimate strain of the element subjected monotonic load, β represents the strength loss ($\beta=0.15$), E is the hysteretic dissipated energy, F_y is the yield load and ID_G and ID are the global and local indices.

A similar analysis was presented in Gómez and Soria (2014) for Motín de Oro and other bridges, but in that paper, it was not considered the random value of the ductility capacity of piers, which was considered as deterministic and evaluated with equation 1. In this work, the variations of mechanical parameters were used to evaluate differences of ductility of piers for each variation of Monte Carlo simulation.

In Figure 4, fragility curves for piers and the entire Motín de Oro bridge are presented for the first seismic scenario, the one with largest PGA; results for other seismic scenarios were not presented by limit space. To obtain these curves, theoretical probabilistic models were adjusted to the results of local and global damage indices of the 300 variations. In this figure, it is observed that the element 12, the far right pier of models of Figure 1, is the element with the largest probability to sustain a damage larger than a certain level. In Figure 1, it is presented the position of each pier according to the color code used for the fragility curves. For example, the probability of a moderate damage, $P[Damage > 0.2/SS1]$, are of 0.26, 0.50 and 0.75 for piers 10, 11 and 12, respectively, being SS1 the first seismic scenario. The global damage of the structure is obtained by using Equation 3. As observed in Figure 4, the probability of a global damage larger than 0.2 (moderate damage) is 0.45; the global index is a mean value of the local indices of the damaged elements. Therefore, if the piers only have damage in the lower side, the global index mean three values, but if the three piers is damaged in both extremes, the global indices is the mean of six values.

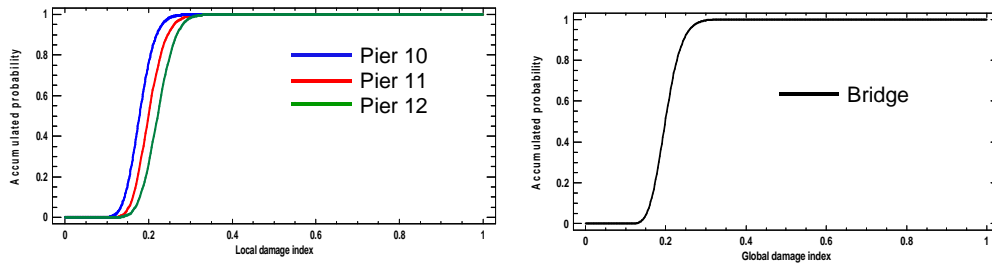


Figure 4– Fragility curves for piers (left) and the bridge (right) for the first seismic scenario

3. Fragility curves of damaged structures

3.1. Damage simulation

As observed in Figure 4, the most vulnerable element for the Motín de Oro bridge is pier 12, the one with the largest probability to suffer a greater certain damage level for the first seismic scenario. In this work, it is assumed that this pier is the one that sustains damage before than the other piers. As it is difficult to assign a specific damage percentage, three qualitative damage levels were used to represent the pier degradation: light, moderate and severe damage. The condition of a RC damaged element for the three damage levels was assumed as a function of experimental results. Specifically, the results of Posada (1994), with experimental analyses of RC columns up to the collapse, were considered.

For a light damage of the pier 12, almost a 10% of degradation, is considered for the case when the concrete cover is lost and the resistance of the element is proportionated by the reinforcing steel and the concrete of the core, confined by stirrups. For moderate and severe damage, more or less 20% and 40% of degradation, some damage is considered in the longitudinal and core concrete materials, then the areas of these elements were degraded under these percentages. A scheme of the degradation of pier 12 for each damage level is observed in Figure 5.

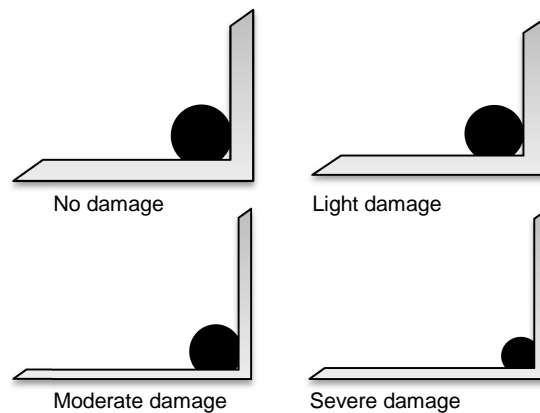


Figure 5 Schemes of the condition of transversal section for different damage levels

For the nonlinear dynamic analyses of the damaged pier, moment-curvature and interaction diagrams are needed. These curves are obtained through analyses with the SAP 2000 program by considering the above commented degradations and the random nature of seismic load and mechanical parameters of Table 1, establishing again 300 variations for the Monte Carlo simulation.

3.2. Fragility curves of damaged bridges

Fragility curves for bridges with a damaged pier are presented in Figures 6 to 8 for light, moderate and severe damage, respectively. These figures show the fragility curves for piers on the left and for the entire bridge on the right. As observed in Figure 6, when light damage is assumed for pier 12, the fragility curves are similar to the ones of Figure 4. For example, $P[Damage > 0.2/SS1]$ are of 0.4, 0.7, 0.1 and 0.22 for piers 10, 11 and 12, and for the bridge, respectively. Then, probability of certain damage is larger for piers 10 and 11, but lower for pier 12, maybe by the difference of theoretical adjusting function.

In Figure 7, when a moderate damage is simulated for pier 12, the fragility curves for not damaged piers (10 and 11) are similar to the not damage option, but for pier 12 the probabilities are larger. For example, $P[Damage > 0.2/SS1]$ are of 0.25, 0.5, 0.98 and 0.9, for piers 10, 11, and 12 and for the bridge, respectively. Although the probabilities of damage of piers 10 and 11 are similar, the greater probability of damage of pier 12 produces an increase of the bridge damage probability. For a single pier bent structure as the Motín de Oro bridge, the failure of a pier is the failure of the system. For a severe damage of pier 12 (Figure 8), similar tendencies are obtained. In this case, the probability of suffer moderate damage for pier 12 is a certain event and the probability of moderate damage in bridge is of 0.95.

In Figure 9 are compared the fragility curves of pier 12, left, and the bridge, right, for different degradations assumed in pier 12 (from not damage to severe damage) for first seismic scenario. As observed in this figure, a light damage produces a minimum movement to the left of the fragility curves, but moderate and severe damage move this curve to the right, especially for severe damage.

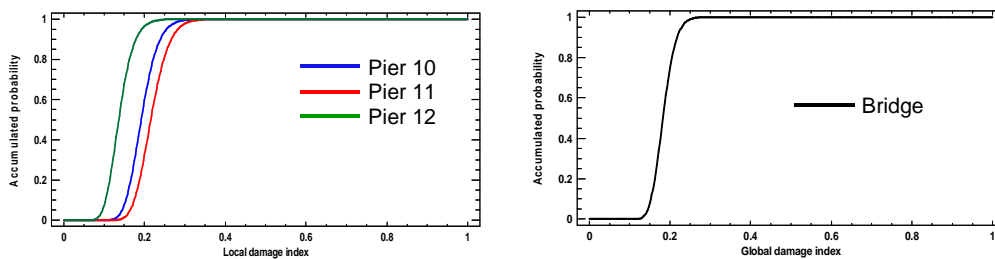


Figure 6– Fragility curves for piers (left) and the bridge (right) for the first seismic scenario. Light damage on pier 12

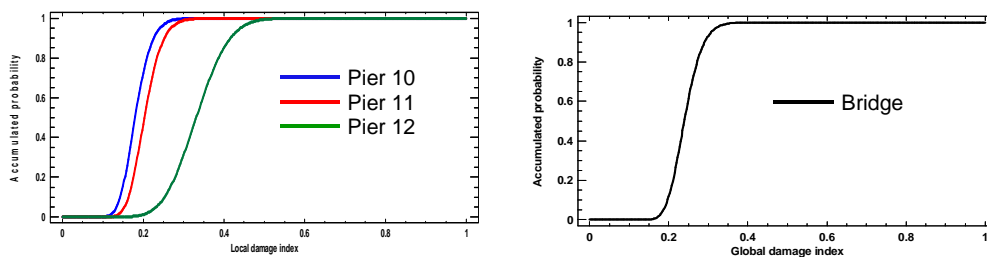


Figure 7– Fragility curves for piers (left) and the bridge (right) for the first seismic scenario. Moderate damage on pier 12

4. Fragility curves for bridge with steel jackets

4.1. Steel jackets for rehabilitation of columns

A steel jacket is a retrofit strategy recommended to increase the volumetric ratio of transverse reinforcement, to increase the ultimate compression strain, to increase passive confinement and allow for a larger rotation capacity of columns. After adding steel jacket, the columns will be stiffer, and the displacement demand along with the plastic rotation demands are expected to decrease (Shafieezadeh *et al.*, 2009). For circular columns two half welded shells of steel plate rolled with a radius larger than the

original transversal section are collocated over the area to be retrofitted, providing a continuous tube with a small gap of cement grout around the column. For rectangular columns, an elliptical jacket is recommended to proportionate a continuous confining action similar to the circular column.

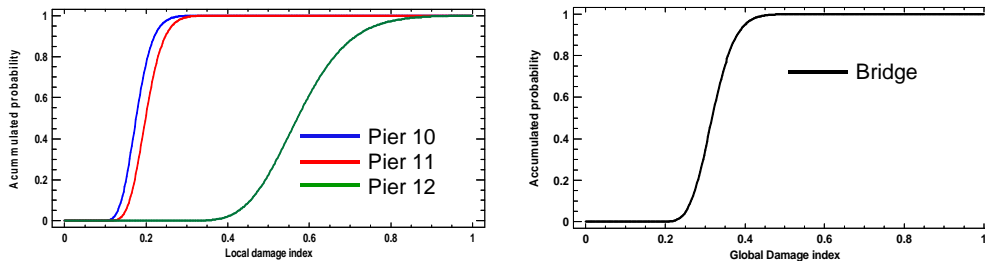


Figure 8– Fragility curves for piers (left) and the bridge (right) for the first seismic scenario. Severe damage on pier 12

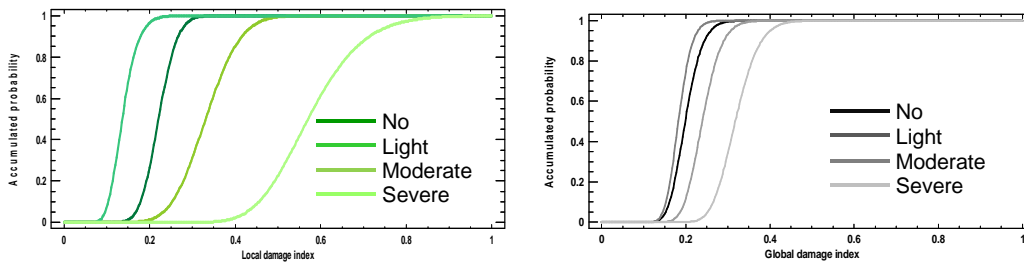


Figure 9– Fragility curves for pier 12 (left) and the bridge (right) for the first seismic scenario. Different damage in pier 12

A procedure of column retrofit design with steel jackets can be consulted in Prietley *et al.*, (2006). This procedure is based on confinement for flexural ductility enhancement, confinement for flexural integrity of column lap splices, shear resistance enhancement, or stiffness considerations, for circular columns or rectangular columns with an elliptical jacket. For Motín de Oro piers, this procedure cannot be used because the piers have wall transversal section. Then, four welded plates were proposed, with a thickness of a compact section that produces a similar fragility curve of the original structure.

4.2. Moment-curvature and interaction diagrams

In the nonlinear analysis of original and damage bridge, moment-curvature and interaction diagrams are defined with SAP 2000 programs, using USER DESIGN option. For retrofitted piers, SAP program was not used, because this code considers a perfect adherence between the original material and the new one.

Moment-curvature diagrams were performed using OpenSees (Mazzoni *et al.*, 2006) in order to determine the capacities of a rectangular reinforced concrete section covered with steel plates. Rectangular patches were used to generate the cross-section: reinforced concrete unconfined region, reinforced concrete confined region, reinforced steel bars and cover steel plates (Figure 10). Patches were discretized into fibers with quadrilateral shapes and a straight line of fibers for reinforced steel bars and four integration points per element.

In model, the implementation of Chang and Mander's concrete model (Concrete 07) with simplified unloading and reloading curves was considered for unconfined and confined regions. The Uniaxial bilinear steel material object with kinematic hardening and optional isotropic hardening described by a non-linear evolution equation was used for reinforced steel bars. The Uniaxial Giuffre-Menegotto-Pinto steel material (Steel 02) with kinematic and isotropic hardening was used in order to provide a realistic representation of the elements response compared to the simpler bi-linear model for steel plates fibers.

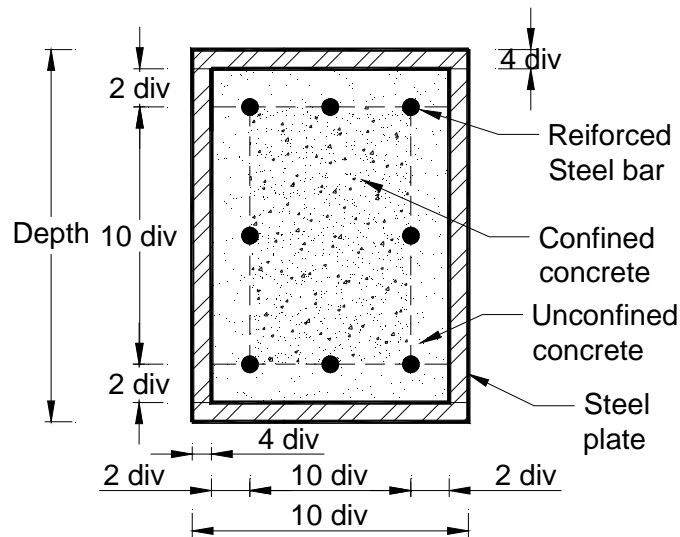


Figure 10. Section definition with OpenSees

To define moment-curvature diagrams, the procedure takes as an input the tag of the section to be analyzed, the axial load P to be applied, the maximum curvature to be evaluated and the number of iterations to achieve the maximum curvature. The procedure first creates the model that consists of two nodes, boundary conditions and a Zero Length Section Element. A single load step is first performed for the axial load, and then the integrator is changed to Displacement Control to impose nodal displacements, which maps directly to section deformations. A reference moment of $M= 1.0$ is defined in a Linear time series. For this reference moment, the Displacement Control obtains the load factor needed to apply the imposed displacement. A node recorder is defined to track the moment curvature results. A load factor is the moment, and the nodal rotation is the curvature of the element with zero thickness (Mazzoni *et al.*, 2006).

To define the interaction diagram, the model consists of two nodes, boundary conditions and a Nonlinear Section Element. Because of the material nonlinearities, an iterative solution is required and a Newton with line search solution algorithm was selected in the program library (Mazzoni *et al.*, 2006) in order to achieve fast convergence. A single load step is performed by using a load control integrator for gravitational load. Here, the time in the domain is set to 0.0 and this load is kept constant. Subsequently, an axial load or a moment are added as static incremental loadings. OpenSees (Mazzoni *et al.*, 2006) was used in this research, because it is capable to simulate the performance of structural and geotechnical systems subjected to lateral loads. Reasonable agreement can be observed between the model and an experimental test to predict the capacity of a member (Uriz and Mahin 2008).

4.3. Fragility curves

In pier 12 a steel jackets were considered with plates of a thickness of 0.64 cm (1/4 in), the minor thickness for a compact section. For light and moderate damage and this retrofit, the local damage index is null for the majority of the 300 variations. Then fragility curves was not elaborated. For pier 12 with a severe damage, almost 40% of degradation, a plate with a thickness of 0.79 cm (5/16 in) yields to a fragility curves that are shown in Figure 11. In this figure, compared with Figure 4, fragility curves for pier 10 and 11 are moved to the right of the original curve, but fragility curve for pier 12 was moved to the left. Now, the probability of a damage larger that a moderate condition, $P[Damage > 0.2/SS1]$, resulted a certain event for piers 10 and 11, but a null event for pier 12. For the whole bridge, this probability is over 0.95.

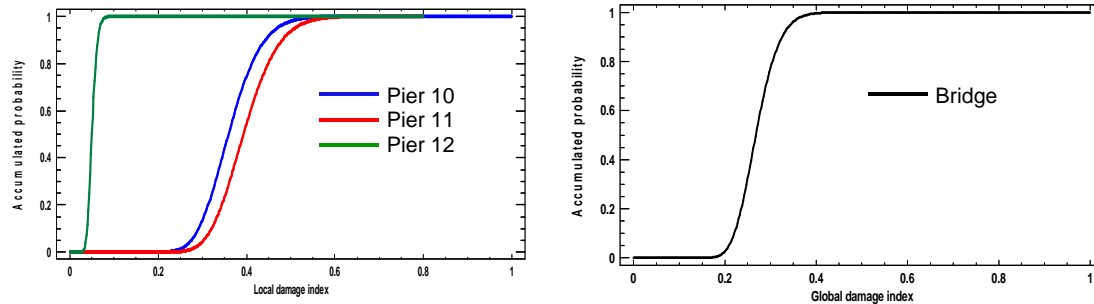


Figure 11– Fragility curves for piers (left) and the bridge (right) for the first seismic scenario. Severe damage on pier 12 with steel jackets

5. Final commentaries

In this paper, fragility curves are used to define the variation of damage probability for the original condition, with some damage condition and when the damage element was retrofitting with steel jackets, for a typical highway bridge in Mexico. The original properties of the bridge piers were the ones considered in design process. To considered damage, the most vulnerable pier of the bridge was degraded to assume light, moderate and severe damage, starting from the results that are obtained in an experimental study of RC columns. Finally, the degraded element was retrofitted with steel jackets, formed by four welded plates, which are a compact section.

When the pier suffers light damage, only the recover concrete was lost and steel plates with small thickness produces null damage in all the variations of Monte Carlo simulations. Then, the use of steel jackets in this condition results excessive, so the replacement of the cover concrete will be sufficient.

When moderate damage was considered, some of the reinforced steel and the concrete were affected. Again, the retrofit of the pier with the small thickness plate produces null damage in most of the 300 variations. Other retrofitting techniques, as concrete jackets, will be less expansive and generate similar results. In addition, partial retrofitting will be considered.

For severe damage and steel jackets with plates with a thickness of 0.79 cm, a larger probability of suffering damage for the not reinforced piers is obtained, but a lower probability for the reinforced element. In this condition, steel jackets was an option, but other techniques will be considered.

Fragility curves are an excellent option to define the variation of damage of piers, considering the uncertainty of the design process. Other reinforced options will be analysed.

6. Acknowledgements

This investigation was partially supported by the Universidad Autónoma Metropolitana (UAM) and the PRODEM organization, part of the Mexican Public Education Secretary. The support of UAM was through an internal project and the PRODEP by the formation of research networks program. Second author express his acknowledgements to CONACYT organization for the grant used to finish his master degree.

7. References

- Carr, A J. "Ruaumoko 3D.Inelastic dynamic analyses", *Civil Engineering Department, University of Canterbury*, 2004.
- Gómez, C. and I. Soria "Vulnerability evaluation of common simple supported bridges", 10th National Conference on Earthquake Engineering, Alaska, USA, Paper No. , 2014.
- Hsiao P-C, D.E. Lehman and C.W. Roeder. A model to simulate special concentrically braced frames beyond brace fracture (2013), *Earthquake Engineering Structures Dynamic*. 42:183–200. doi: 10.1002/eqe.2202.
- Karim, K. R., and Yamazaki, f. "Comparison of empirical and analytical fragility curves for RC bridges in Japan", *8th ASCE Special Conference on Probabilistic Mechanics and Structural Reliability*, 2000.

- Liao, W., and Loh, C. "Preliminary study on the fragility curves for highway bridges in Taiwan", *Journal of the Chinese Institute of Engineering*, Vol. 27, No. 3, 2004, pp. 367-375.
- Mackie, K. R., Nielson, B. G. "Uncertainty quantification in analytical bridge fragility curves", *Lifeline Earthquake in a Multi-hazard Environment*, ASCE, 2009, 148.206.91.180.
- Mazzini, S., F. McKenna, M. Scott, M y G. Fences (2006). Open system for earthquake engineering simulation, user command-language manual, Report NEES grid-TR 2004-21. Pacific Earthquake Engineering Research, University of California, Berkeley, CA.
- Nasseradesadi, K, Ghafory-Ashtiany, M., Eshghi, S., and Zolfaghari, M. R. "Developing seismic fragility functions of structures by stochastic approach". *Asian Journal of Civil Engineering*, Vol. 10, No.2. 2009, pp.183-200.
- Nielson, B. G., and DesRoches, R. "Analytical seismic fragility curves for typical bridges in the central and Southeastern United States", *Earthquake Spectra*, Vol. 23, No. 3, 2007, pp. 615-633.
- Olmos, B., Jara, J. M., Gómez, C., and M. Jara "Seismic response of bridges with a pier substructure reinforced with steel jacketing" *5as Jornadas Portuguesas de Engenharia de Estruturas*, JPEE, Paper 136, Portugal, 2014.
- Padgett, J. E., and DesRoches, R. "Methodology for the development of analytical fragility curves for retrofitted bridges", *Earthquake Engineering and Structural Dynamics*, No. 37, 2008, pp. 1157-1174. DOI:10.1002/eqe.801m.
- Park, Y. J., and Ang, A. H. "Mechanistic seismic damage model for reinforced concrete", *Journal of Structural Division (ASCE)*, Vol. 111, No. 4, 1985, pp. 722-739.
- Posada B. "La degradación del concreto armado". *Revista Universidad EAFIT*, Colombia. Vol. 30, No. 93, pp. 16-20, 1994.
- Priestley, M. J., and Park, Y. J. "Strength and ductility of concrete bridge columns under seismic loading", *ACI Structural Journal*, Technical Paper, Title No. 84-S8, 1989.
- Priestley, M. J. N., Seibel, F. and Calve, G. M. "Seismic design and retrofit of bridges", John Wiley & Sons, New York, USA, 1996.
- SAP2000, Advanced 14.1, integrated solution for structural analyses and design, Computer and Structures INC. 2000.
- Shafieezadeh, A., Hu, W., E. Erduran and K. L. Ryan "Seismic vulnerability assessment and retrofit recommendations for state highway bridges: case studies" *Utah Department of Transportation Research Division, Report UT-0908*, 2009.
- Uriz P. y Mahin, S. (2008). Toward Earthquake-Resistant Design of Concentrically Braced Steel-Frames Structures, Report of Pacific Earthquake Engineering Research Center, PEER 2008/08, November.
- Zhang, J Y, Huo, S., Brandenburg, J., and Kashighadi, P. "Effects of structural characterization on fragility functions of bridges subjected to seismic shaking and lateral spreading", *Earthquake Engineering and Engineering Vibrations*, Vol. 7, No. 4, 2008, pp. 369-382, DOI: 10.1007/s 1803.008.1009-2.